SAND2018-9647J

Proactive Operations and Investment Planning via Stochastic Optimization to Enhance Power Systems Extreme Weather Resilience

Michael Bynum[1,2], Andrea Staid[1], Bryan Arguello[1], Anya Castillo[1], Jean-Paul Watson[3], and Carl D. Laird[1,2]

[1]Sandia National Laboratories, Albuquerque, NM, 87185 USA
[2]Davidson School of Chemical Engineering, Purdue University, West Lafayette, IN, 47907 USA
[3]Sandia National Laboratories, Livermore, CA, 94550 USA
[4]mlbynum@sandia.gov, astaid@sandia.gov, barguel@sandia.gov, arcasti@sandia.gov, jwatson@sandia.gov, cdlaird@sandia.gov

August 29, 2018

Abstract

We present novel stochastic optimization models to improve power systems resilience to extreme weather events. We consider proactive redispatch, transmission line hardening, and transmission line capacity increases as alternatives for mitigating expected load shed due to extreme weather. Our model is based on linearized or "DC" optimal power flow, similar to models in widespread use by independent system operators (ISOs) and regional transmission operators (RTOs). Our computational experiments indicate that proactive redispatch alone can reduce the expected load shed by as much as 25% relative to standard economic dispatch. This resiliency enhancement strategy requires no capital investments and is implementable by ISOs and RTOs solely through operational adjustments. We additionally demonstrate that transmission line hardening and increases in transmission capacity can, in limited quantities, be effective strategies to further enhance power grid resiliency, although at significant capital investment cost. We perform a cross validation analysis to demonstrate the robustness of proposed recommendations. Our proposed model can be augmented to incorporate a variety of other operational and investment resilience strategies, or combination of such strategies.

1 Introduction

The United States Presidential Policy Directive 21 (PPD-21) originally outlined the nation's need for secure and resilient critical infrastructure and identified 16 critical infrastructure sectors, including the electric power sector [13]. Subsequently, national focus on improving critical infrastructure resiliency has only increased. In particular, the resilience of electric power systems is vital for both the economy and public health and safety. Physical components of power systems may be damaged by natural disasters (e.g., earthquakes and hurricanes) and by intentional acts (e.g., perpetrated by nation-state actors), ultimately impacting the ability to deliver power to consumers. The annual cost of power outages due to severe weather in the United States alone between 2003 and 2012 is estimated to be between $18 billion to $33 billion USD [8].

Informally, resilience refers to the ability of a system to withstand and quickly recover from adverse events [32]. Here, we specifically focus on power systems resilience to severe weather events, e.g., hurricanes and

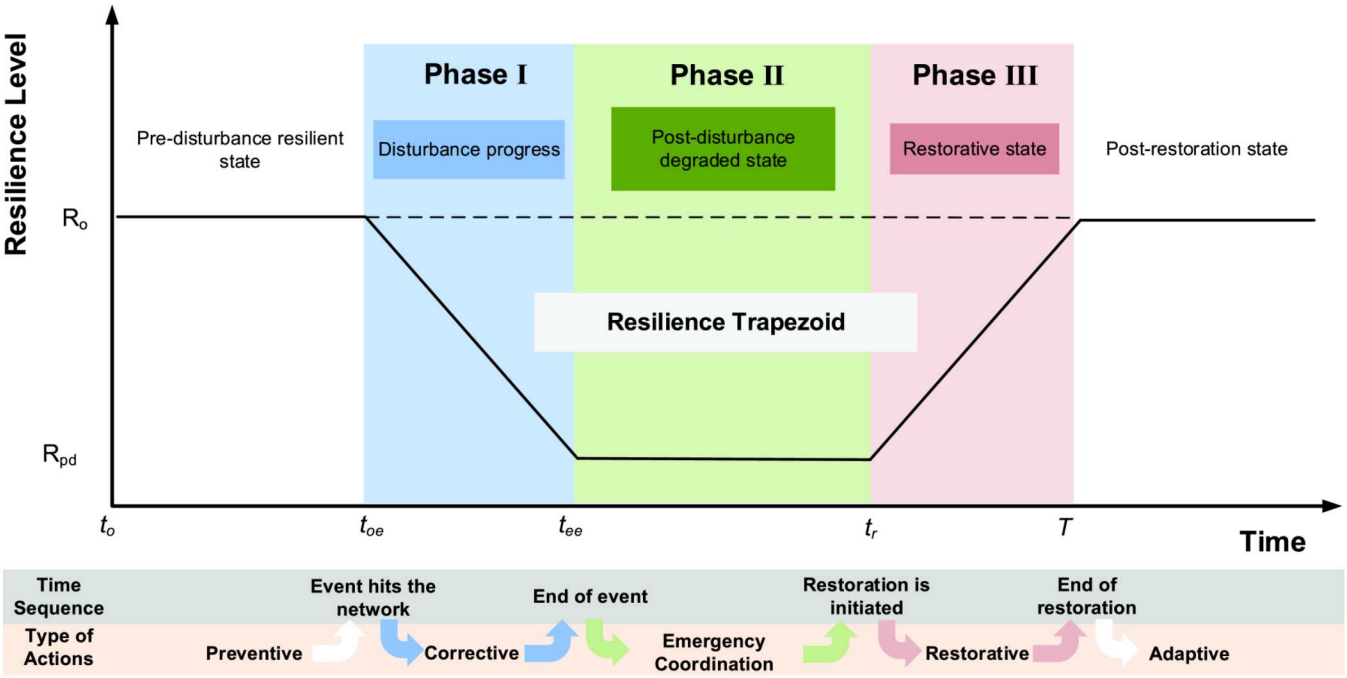

Fig. 1. Resilience Trapezoid

ice storms. A necessary first step toward improving power system resilience to such events is estimating the impact of these events on power systems. Such estimation involves weather forecasting, predicting the effect of severe weather conditions on power system components, and modeling the performance (operations) of power systems given sets of damaged components [10, 16–18].

Panteli et al. [19] describe the concept of a "resilience trapezoid" toward evaluation and quantification of critical infrastructure resilience. The resilience trapezoid, illustrated in Figure 1, highlights the performance of a system during an adverse event (Phase I), immediately following an adverse event (Phase II), and during the restoration process (Phase III). Panteli et al. [19] subsequently introduced the $\Phi\Lambda E\Pi$ resilience metric system based upon the different phases of the resilience trapezoid. The $\Phi\Lambda E\Pi$ resilience metric system is composed of four components:

- Φ: The slope of system performance during Phase I
- Λ: The amount by which performance drops from Phase I to Phase II (i.e., the baseline resilience minus the post-disturbance resilience: $R_0 - R_{pd}$)
- E: The duration of Phase II
- Π: The slope of the system performance during Phase III

The $\Phi\Lambda E\Pi$ metric system provides a conceptual framework for categorizing different approaches to improving resilience.

In the context of power systems operations, the primary considerations for Phase I of the resilience trapezoid are minimization of unserved demand due to component damage and the prevention of cascading outages (i.e., blackouts). Cascading outages are complex phenomena due to the complex interactions between system components, component failures, and protection schemes. Many different failure types may contribute to a blackout, including cascading overloads, transient instabilities, and voltage collapse [3].

Typical mitigation strategies include remedial action schemes such as generation trip, brake insertion, fast valve/gen ramp, HVDC ramp, islanding, intentional load shed, excitation forcing, shunt capacitor/reactor switching, and series capacitor/reactor switching [26]. Chen et al. [6] propose a decision-event tree to help operators respond rapidly to an event and prevent cascading outages. Wide area monitoring and backup protection systems have also been proposed for preventing blackouts [25, 35]. Song and Kezunovic [23] present an early detection scheme that uses the vulnerability index, margin index, and power flow solutions to predict possible failures. Cascading outages may also be prevented by partitioning the network into islands by minimal cut sets [28] and using graph partitioning methods in the context of mixed-integer linear programming (MILP) models [9].

Extensive research has been conducted to develop improved strategies for post-blackout restoration (Phase III). Wang et al. [29] divide restoration into three stages (preparation, system restoration, and load restoration) and provide a review of research conducted to address each stage. Preparation primarily involves identification of the status of various system components [1]. System restoration deals with restarting generators and reconnecting and synchronizing the power grid. For example, Sun et al. [24] propose a MILP model to determine an optimal generator restart sequence in order to maximize system generation capability. Load restoration (also known as distribution system restoration) deals with scheduling load pickup while maintaining system frequency. This process must be coordinated with generation capability [1, 29].

In this paper, we focus on optimization-based strategies for demonstrably improving the performance of power systems in Phase II, i.e., increasing the post-disturbance resilience R_{pd}. Many hardening options are available to achieve this goal, including hardening transmission lines, elevating substations, the addition of distributed generation, the introduction of storage devices, and system network reconfiguration (e.g., switching) [19]. Computational approaches are generally required to rigorously select from among these various options. Zare et al. [34] introduce a stochastic MILP optimization model for switch placement in power distribution systems in order to isolate faulted areas; network flows are not considered. In general, determining which option, or combination of options, is computationally challenging, driving research toward more efficient approaches. Panteli et al. [19] propose hardening transmission lines according to each corridor's Resilience Achievement Worth (RAW) index. Wang et al. [30] perform Monte Carlo sampling to assess line outage impacts on generation unit scheduling. However, such heuristic approaches to improving resilience generally do not generally provide optimal solutions. They may provide significantly worse-than-optimal solutions in the presence of a diverse set of strategies and large system sizes.

Alternatively, rigorous optimization approaches based on mathematical programming can provide optimal solutions in these contexts, although the computational challenges can be significant. This difficulty is illustrated in the body of literature on bi-level and tri-level optimization models and corresponding solution algorithms for critical infrastructure defense planning [2, 21, 33]. These models consider critical infrastructure defense strategies in the context of an intelligent adversary, and focus on mitigating worst-case impacts to a power system. For example, Shao et al. [22] and Wang et al. [27] use similar strategies to mitigate the impact of component failures (contingencies) within the context of long-term (i.e., investment) and short-term (i.e., operations) planning, respectively. The former introduces a two-stage tri-level optimization model and imposes an upper limit on load shed. The latter introduces a two-stage robust optimization model to minimize a linear combination of operating cost and load shed, focusing again on the worst-case loss induced by component failure. Both of these models are solved using decomposition strategies in which the model is partitioned into a MILP master problem and bi-level subproblems. The bi-level subproblems (which are typically more computationally demanding) are used to find the worst-case contingencies, which are iteratively integrated into the master problem. Hardening strategies recommended by such models are designed to be effective against an omniscient adversary with full knowledge of the power system under consideration, e.g., a nation state actor.

The above and related optimization models are not appropriate for mitigating the impact of extreme weather on power systems, where component failures are strongly a function of geography and typically

highly correlated. To improve power systems resilience to extreme weather events, we instead propose a novel optimization model that explicitly considers a range of possible component outages due to extreme weather events. Specifically, we introduce a two-stage stochastic MILP optimization model – based on linearized or "DC" power flow, of the type widely used in power systems operations – whose solution determines optimal dispatch and / or investment planning in the first stage (pre-storm) to minimize the expected load shed due to system component damage from different realizations of a second-stage extreme weather event. We demonstrate the utility of our stochastic MILP model on both small (30 bus) and large (2383 bus) benchmark power systems. Although not detailed here, we note that we performed similar analyses with a large-scale, proprietary utility, yielding qualitatively identical results; these analyses drove the development of the stochastic MILP model presented herein. We also perform a cross validation analysis that demonstrates our model can yield a near-optimal solution (with respect to out-of-sample performance) considering less than 0.001% of all possible outage realizations.

The remainder of this paper is organized as follows. In the following section, we describe strategies for generating extreme weather outage realizations (i.e., scenarios) and briefly discuss data challenges associated with these strategies. We then present our stochastic MILP model for improving power system resiliency to sampled extreme weather outage scenarios. Subsequent sections then detail (1) computational results obtained with our stochastic MILP model considering both small and large benchmark power systems and (2) cross validation results illustrating the robustness of our solutions, which can be obtained using only a small fraction of all probable component outage scenarios. We then conclude by summarizing our contributions and discuss extensions for future research.

2 Scenario Construction

We construct a set of relevant probabilistic scenarios that capture transmission line outages (e.g., due to damage or de-energization) associated with extreme weather event(s) of interest. These scenarios are used as a key input to our stochastic MILP optimization model, and explicitly represent uncertainty regarding future possible realizations of component damage associated with adverse weather conditions. We note that these scenarios can be associated with a specific operational event (e.g., an oncoming hurricane) or a set of adverse events common to a specific region (e.g., ice storms and high winds), when considering system planning.

Ideally, such scenarios would be obtained from statistical models representing system component outages, constructed (e.g.,) using historical component failure data. For the synthetic test systems we consider here, we instead construct scenarios by first sampling the number of transmission line outages from a negative binomial distribution, and then determine which lines were not in service by sampling from a uniform distribution.

For our real-world utility case study, extensive historical component failure data was available. Using this data, we first determined the probability of an outage for each transmission line due to specific weather-related failures. Most regions of a power system historically have very few to no observed outages. When no priors were available, we estimated failure probabilities based on the average failure probability across all transmission lines in the network that are operating at the same voltage level. Regions that are more prone to certain types of weather hazards due to equipment age, geographical location, and/or line routing commonly have a disproportionate number of weather-related outages. We apply the calculated probabilities to simulate such failures on each transmission line and construct a set of scenarios comprised of both 'standard' and 'extreme' weather events. We determine the standard scenarios through random sampling of the associated failure probabilities for each transmission line. This approach results, on average, in very few failures. In contrast, we create the extreme scenarios by sampling for a target number of outages that is equivalent to the number of lines failures observed in historical data from significant weather events. These extreme scenarios model the "tail" of the distribution, and represent low-probability but still observed weather conditions.

For example, such extreme scenarios have dozens to hundreds of outages that historically occurred in the real-world utility's power system.

3 Stochastic Programming Models for Enhancing Resiliency

We now present a series of two-stage stochastic optimization models to improve power systems resilience to extreme weather events. We begin by briefly reviewing key concepts in power systems modeling, specifically the linearized or "DC" approximation of power flow. We then introduce a stochastic linear program (LP), without discrete decision variables, to optimally and proactively redispatch generators in advance of an extreme weather event. Subsequently, we extend this base stochastic LP model to consider various capital investment strategies for improving resiliency, specifically transmission line hardening and increases in transmission line capacity. The latter options involve the introduction of binary (i.e., discrete) decision variables into our optimization model, resulting in a more difficult stochastic MILP.

3.1 Linearized Power Flows

Power systems are modeled as a network of nodes and links. In this case, the nodes represent buses, and the links represent branches (transmission lines and/or transformers). We use a common linearization of the transmission line generalized π-model referred to as the DC approximation. This linearization assumes that the resistance of each transmission line is much less than its reactance, the voltage magnitude at each bus is close to nominal (i.e., 1 in the per unit system), and the voltage angle difference between interconnected buses is small [36]. These assumptions result in the following linear angle-to-power relationship to define the real power flow on line k:

$$p_k = \frac{1}{X_k T_k}\left(\theta_b - \theta_n - \Theta_k^{\text{shift}}\right) \qquad \forall (k,b,n) \in \mathcal{L} \tag{1}$$

where $\mathcal{L}$ is the set of triplet indices including line k, and its interconnected buses b and n; X_k, T_k, and Θ_k^{shift} are the reactance, transformer tap ratio, and transformer phase shift of branch k, respectively; and θ_b and θ_n are the voltage angles at the "from" and "to" buses of branch k, respectively. The real power flow p_k is limited by

$$-S_k^{\max} \le p_k \le S_k^{\max} \qquad \forall k \in \mathcal{K} \tag{2}$$

where $S_k^{\max}$ is the transfer capacity of line k. Additionally, the power transfer between interconnected buses b and n can be limited by the maximum voltage angle difference $\Theta_{(b,n)}^{\max}$ in

$$-\Theta_{(b,n)}^{\max} \le \theta_b - \theta_n \le \Theta_{(b,n)}^{\max} \qquad \forall (b,n) \in \mathcal{A} \tag{3}$$

where $\mathcal{A}$ is a set of adjacent bus pairs.

Buses may have shunts, loads, and/or generators. An energy balance at each bus b requires

$$\sum_{g \in \mathcal{G}_b} p_g^G + \sum_{k \in \mathcal{K}_b^{in}} p_k - \sum_{k \in \mathcal{K}_b^{out}} p_k = P_b^L + G_b^S \qquad \forall b \in \mathcal{B} \tag{4}$$

where $\mathcal{B}$ is the set of all buses, $\mathcal{G}_b$ is the set of generators at bus b, $\mathcal{K}_b^{in}$ is the set of all transmission lines with bus b as its "to" bus, $\mathcal{K}_b^{out}$ is the set of all transmission lines with bus b as its "from" bus, p_g^G is the real component of the power generated at generator g, P_b^L is the real component of the power demand at bus b, p_k is the real component of the power flowing along transmission line k, and G_b^S is the shunt conductance at bus b.

3.2 Resilient Dispatch Formulation

We now present our two-stage stochastic LP model to optimally dispatch generators in preparation for extreme weather events. The first decision stage of the model captures steady state power system operations prior to the event. The second decision stage represents post-event steady-state operation following a number of component outages due to the event. For simplicity, we only consider transmission line outages; the model can be generalized to consider bus and generator outages as well. Any first stage (proactive dispatch) decisions must be made before any uncertainty is revealed, and are therefore *non-anticipative*. Uncertainty is revealed between decision stages one and two. Decisions (reactive dispatch and load shed) in stage two are known as *recourse* decisions, as they are made following realization of any potential uncertainties – in our case, component outages. As described previously, this uncertainty is captured via a finite number of discrete scenarios, each with a (potentially distinct) probability of occurrence.

Generator ramping rates are the key linkage between the first and second decision stages; operational characteristics of thermal generators dictate that they can only feasibly change power output levels at a limited rate. In this context, the optimization objective is to identify a first stage dispatch that minimizes the expected load-shed across the set of extreme event scenarios $\mathcal{S}$. The second stage decisions can be viewed loosely as a "play book" – if a scenario $s \in \mathcal{S}$ is realized, then the optimal action to minimize load shed is to re-dispatch according to the recourse p_g^G values.

Our model, which we refer to as the Resilient Dispatch Formulation (RDF), is

$$\min \sum_{s\in\mathcal{S}} \Omega_s \Big(\sum_{b\in\mathcal{B}} p_{b,s}^{L,shed} + \alpha \sum_{g\in\mathcal{G}} p_{g,s}^{G,cur} \Big) \tag{5a}$$

s.t.

$$\sum_{g\in\mathcal{G}_b} p_{g,0}^G + \sum_{k\in\mathcal{K}_b^{\text{in}}} p_{k,0} - \sum_{k\in\mathcal{K}_b^{\text{out}}} p_{k,0} = P_b^L + G_b^S \qquad \forall b \in \mathcal{B} \tag{5b}$$

$$P_g^{G,\min} \le p_{g,0}^G \le P_g^{G,\max} \qquad \forall g \in \mathcal{G} \tag{5c}$$

$$p_{k,0} = \frac{1}{X_k T_k}(\theta_{b,0} - \theta_{n,0} - \Theta_k^{\text{shift}}) \qquad \forall (k,b,n) \in \mathcal{L} \tag{5d}$$

$$-S_k^{\max} \le p_{k,0} \le S_k^{\max} \qquad \forall k \in \mathcal{K} \tag{5e}$$

$$-\Theta_{(b,n)}^{\max} \le \theta_{b,0} - \theta_{n,0} \le \Theta_{(b,n)}^{\max} \qquad \forall (b,n) \in \mathcal{A} \tag{5f}$$

$$-P_g^{G,R} \le p_{g,0}^G - p_{g,s}^G \le P_g^{G,R} \qquad \forall g \in \mathcal{G} \;\; \forall s \in \mathcal{S} \tag{5g}$$

$$\theta_{\text{ref},0} = 0 \tag{5h}$$

$$\sum_{g\in\mathcal{G}_b} \left(p_{g,s}^G - p_{g,s}^{G,cur} \right) + \sum_{k\in\mathcal{K}_b^{\text{in}}} p_{k,s} - \sum_{k\in\mathcal{K}_b^{\text{out}}} p_{k,s} = P_b^L - p_{b,s}^{L,shed} + G_b^S \qquad \forall b \in \mathcal{B}, \forall s \in \mathcal{S} \tag{5i}$$

$$P_g^{G,\min} \le p_{g,s}^G \le P_g^{G,\max} \qquad \forall g \in \mathcal{G}, \forall s \in \mathcal{S} \tag{5j}$$

$$p_{k,s} = \frac{1}{X_k T_k}(\theta_{b,s} - \theta_{n,s} - \Theta_k^{\text{shift}}) \qquad \forall (k,b,n) \in \mathcal{L}\backslash\mathcal{L}_s, \forall s \in \mathcal{S} \tag{5k}$$

$$p_{k,s} = 0 \qquad \forall k \in \mathcal{K}_s \;\; \forall s \in \mathcal{S} \tag{5l}$$

$$-S_k^{\max} \le p_{k,s} \le S_k^{\max} \qquad \forall k \in \mathcal{K}, \forall s \in \mathcal{S} \tag{5m}$$

$$-\Theta_k^{\max} \le \theta_{b,s} - \theta_{n,s} \le \Theta_k^{\max} \qquad \forall (b,n) \in \mathcal{A}_s, \forall s \in \mathcal{S} \tag{5n}$$

$$\theta_{\text{ref},s} = 0 \qquad \forall s \in \mathcal{S} \tag{5o}$$

$$0 \le p_{b,s}^{L,shed} \le P_b^L \qquad \forall b \in \mathcal{B}, \forall s \in \mathcal{S} \tag{5p}$$

$$0 \leq p^{G,cur}_{g,s} \leq p^{G}_{g,s} \qquad \forall g \in \mathcal{G}, \forall s \in \mathcal{S} \tag{5q}$$

where constraints (5b) – (5f) are related to first stage decisions and are denoted by the index 0, constraints (5i) – (5q) are related to second stage decisions and are denoted by scenario s, and constraint (5g) enforces the ramping capability for all generators from the nominal operating state in the first stage to the outage state in the second stage.

The objective function, (5a), is to minimize the sum of the load shed and the over-generation. The over-generation term is needed for feasibility (e.g., generators may become islanded). Constraints (5b) and (5i) represent the nodal real power balance at every bus. Constraints (5c) and (5j) limit the real power output at each generator. Constraints (5d) and (5k) determine the real power flow on each line k between interconnected buses b and n, where $\mathcal{L}\backslash\mathcal{L}_s$ denotes all transmission lines that are in service in scenario s. For the transmission line outages in scenario s, constraint (5l) enforces zero real power flow. Constraints (5e) and (5m) limit the real power flow on each transmission line, and constraints (5f) and (5n) limit the voltage angle difference between connected buses. Since an infinite number of solutions exist for equivalent voltage angle differences $\theta_b - \theta_n$ over all $(b, n) \in \mathcal{A}$, constraints (5h) and (5o) set the voltage angle at the reference bus (denoted with subscript "ref") to determine a single solution. For each adverse weather event scenario s, constraint (5p) limits the nonnegative load shed below the specified load, P^{L}_{b}, and constraint (5q) limits the nonnegative curtailment needed below the generator's operating level, $p^{G}_{g,s}$. The generator curtailment constraint approximates the more realistic model in which generators either shut-down or operate at an output between the minimum operating level (MOL), $P^{G,\min}_{g}$, and its maximum capacity, $P^{G,\max}_{g}$.

The RDF is applicable for hours to days before a severe weather event to obtain a resilient dispatch for a given weather forecast that is used to construct scenarios (see Section 2). The resilient dispatch may be less efficient than the economic dispatch used in standard operating conditions. However, the RDF operates the generators in a state that enables transition to contingency states with as little load shedding and generator curtailment as possible. Additionally, because the problem is entirely continuous and linear, it may be solved efficiently with commercial solvers such as Gurobi [11] and CPLEX [14] in the short time frame between weather forecasts and actual weather events.

3.3 Extensions for Long Term Investments

The RDF can be extended to consider many possible long term planning investments for improved grid resilience. Possible investments for improving resilience include hardening transmission lines, elevating substations, increasing transmission capacity, placing switches for transmission switching, and many others. All of these could be modeled within a stochastic programming framework. We demonstrate the extensibility of the RDF with the following two examples: (1) transmission line hardening and (2) increasing transmission capacity.

3.3.1 Hardening Transmission Lines

Transmission lines can be hardened to severe weather. A few possible hardening strategies include burying transmission lines underground, installing guy wires, and upgrading crossarm materials [29]. However, it is unreasonable to harden every component in the network. Therefore, it is important to understand the priority of lines to be hardened and the impact of this investment on grid resiliency.

Therefore, we augment the RDF in (5) to optimally determine the set of branches to harden for a given budget. We introduce a binary variable, δ_k, to indicate whether a transmission line is hardened ($\delta_k = 1$) or not ($\delta_k = 0$). The assumption is that once a line is hardened, it becomes invulnerable to the current weather event. We replace constraints (5k) – (5n) as follows:

$$p_{k,s} = \frac{1}{X_k T_k}(\theta_{b,s} - \theta_{n,s} - \Theta^{\text{shift}}_{k}) \qquad \forall (k, b, n) \in \mathcal{L}\backslash\mathcal{L}_s, \forall s \in \mathcal{S} \tag{6a}$$

$$
\begin{aligned}
&- M(1-\delta_k) \le p_{k,s} X_k T_k - \\
&\quad (\theta_{b,s} - \theta_{n,s} - \Theta_k^{\text{shift}}) \le M(1-\delta_k) && \forall (k,b,n) \in \mathcal{L}_s, \forall s \in \mathcal{S} && \text{(6b)}\\
&- S_k^{\max} \le p_{k,s} \le S_k^{\max} && \forall k \in \mathcal{K} \backslash \mathcal{K}_s, \forall s \in \mathcal{S} && \text{(6c)}\\
&- S_k^{\max} \delta_k \le p_{k,s} \le S_k^{\max} \delta_k && \forall k \in \mathcal{K}_s, \forall s \in \mathcal{S} && \text{(6d)}\\
&- \Theta_{(b,n)}^{\max} \le \theta_{b,s} - \theta_{n,s} \le \Theta_{(b,n)}^{\max} && \forall (b,n) \in \mathcal{A}_s, \forall s \in \mathcal{S} && \text{(6e)}\\
&- \Theta_{(b,n)}^{\max} - M(1-\delta_k) \le \theta_{b,s} - \theta_{n,s} \le \Theta_{(b,n)}^{\max} + M(1-\delta_k) && \forall (k,b,n) \in \mathcal{L}_s, \forall s \in \mathcal{S} && \text{(6f)}\\
&\sum_{k \in \mathcal{K}} \delta_k \le C && && \text{(6g)}\\
&\delta_k \in \{0,1\} && \forall k \in \mathcal{K} && \text{(6h)}
\end{aligned}
$$

Constraint (6a) is the real power flow for in-service lines, and constraint (6b) enables real power flow for transmission line outages that have been hardened using Big-M notation. Constraint (6d) enforces the transfer capacity limits on hardened lines, and otherwise prevents power flow on lines that remain in an out of service state. In other words, constraint (6b) results in an unconstrained voltage angle difference when constraint (6d) is inactive. Then constraint (6e) enforces the voltage angle difference limits between connected buses, and constraint (6f) only enforces this limit when there exists a hardened line out of the set of outages for interconnections between buses b and n in scenario s. Constraint (6g) limits the number of hardened transmission lines to C. Constraint (6h) defines the first-stage binary variable δ_k.

3.3.2 Increasing Transmission Capacity

An alternative hardening investment is to increase the pre-existing transmission capacity. In this case, we introduce a binary variable, γ_k, to represent whether the capacity of the corresponding transmission line has been increased ($\gamma_k = 1$) or not ($\gamma_k = 0$). Constraint (5m) is replaced by the following:

$$
\begin{aligned}
&- S_k^{\max}(1-\gamma_k) - \Lambda S_k^{\max} \gamma_k \le p_{s,k} \le S_k^{\max}(1-\gamma_k) + \Lambda S_k^{\max} \gamma_k && \forall k \in \mathcal{K} \;\; \forall s \in \mathcal{S} && \text{(7a)}\\
&\sum_{k \in \mathcal{K}} \gamma_k \le C && && \text{(7b)}\\
&\gamma_k \in \{0,1\} && \forall k \in \mathcal{K} && \text{(7c)}
\end{aligned}
$$

where Λ is the factor by which the transmission capacity will be increased. Constraint (7a) enforces the nominal capacity limits when $\gamma_k = 0$, and increases the limits by a factor of Λ when $\gamma_k = 1$. Constraint (7b) limits the number of transmission lines for which the thermal limits can be increased. Constraint (7c) defines the first-stage binary variable γ_k.

4 Computational Results

The stochastic programming formulations (RDF, THF, and TCF) presented in Section 3 were successfully applied to a large real-world utility with scenarios constructed as discussed in Section 2. However, the data and results are proprietary, so we instead present results from two standard test cases from the publicly available Matpower software package for power flow analysis: case30 and case2383wp [36].

The network sizes for the test cases and the proprietary utility are summarized in Table 1. One hundred scenarios were used for case30, and fifty scenarios were used for case2383wp. The number of transmission line outages in each scenario was drawn from a negative binomial distribution, and the transmission lines that were out of service were drawn from a uniform distribution. The resulting problem sizes for the Resilient Dispatch Formulation (RDF), Transmission Hardening Formulation (THF), and Transmission Capacity Formulation (TCF) are given in Table 2.

Table 1. Summary of network sizes

	case30	case2383wp	Proprietary Utility
# of Buses	30	2383	$O(10,000)$
# of Generators	6	327	$O(1,000)$
# of Transmission Lines	41	2896	$O(10,000)$

Table 2. Problem size statistics

Test Case	Formulation	Continuous Variables	Binary Variables	Equality Constraints	Inequality Constraints
case30	RDF	9,677	0	6,662	8,664
case30	THF	14,579	41	10,762	11,613
case30	TCF	13,777	41	10,762	10,189
case2383wp	RDF	390,755	0	267,767	341,639
case2383wp	THF	537,401	2,896	412,567	347,950
case2383wp	TCF	535,555	2,896	412,567	344,820
Utility	RDF	1,583,730	0	1,279,810	100,882
Utility	THF	1,635,443	972	1,313,286	141,531
Utility	TCF	1,625,018	1,588	2,122,236	182,176

The stochastic programming formulations were modeled with Pyomo [12] and solved with CPLEX [14]. The THF and TCF formulations for case30 were solved to less than a 0.01% optimality gap. The THF problems for case2383wp were solved to less than a 2% gap, and the TCF formulations for case2383wp were solved to less than a 4% gap. The weight α on the generator curtailment term in the objective was 0.01. The value of Λ used in the TCF formulation was 2. Due to a lack of ramp rate data for the synthetic test cases, a correlation was developed between the maximum power output of the generator and the ramp rate using real proprietary utility data. The correlation was then used to estimate ramp rates for these cases. A conservative 5-minute ramp rate was used in order to limit the overall change of the state of the grid during the severe weather event because the system dynamics were not modeled.

The results are presented in Figures 2 and 3; incremental variants variants are shown in Figures 4 and 5. The left and right panels illustrate results for the THF and TCF formulations, respectively. The y-axis indicates the expected load shed $\mathbb{E}\left(p^{L,shed}\right)$ across all scenarios, i.e.,

$$\mathbb{E}\left(p^{L,shed}\right) = \sum_{s\in\mathcal{S}} \Omega_s \sum_{b\in\mathcal{B}} p_{b,s}^{L,shed}$$

in the objective function (5a). The asterisk represents the *baseline*, which is the case where no preparation is done before the severe weather event. Rather, the generator outputs in the first stage are fixed (as determined by economic dispatch), and the expected load shed is simply the evaluation of the effect of each scenario on the system. Note that when the number of lines hardened is zero, this corresponds to the RDF solution (redispatch only). The same is true for the TCF figure (i.e., optimal value at zero is the RDF solution).

The RDF results in Figures 4 and 5 indicate that simply redispatching generators before a severe weather event reduces the expected load shed by 25.0% and 16.6% for case30 and case2383wp, respectively. We note that the incremental reduction in expected load shed is calculated as the percentage with respect to the baseline load shed. This substantial reduction in load shed does not require any capital investments and

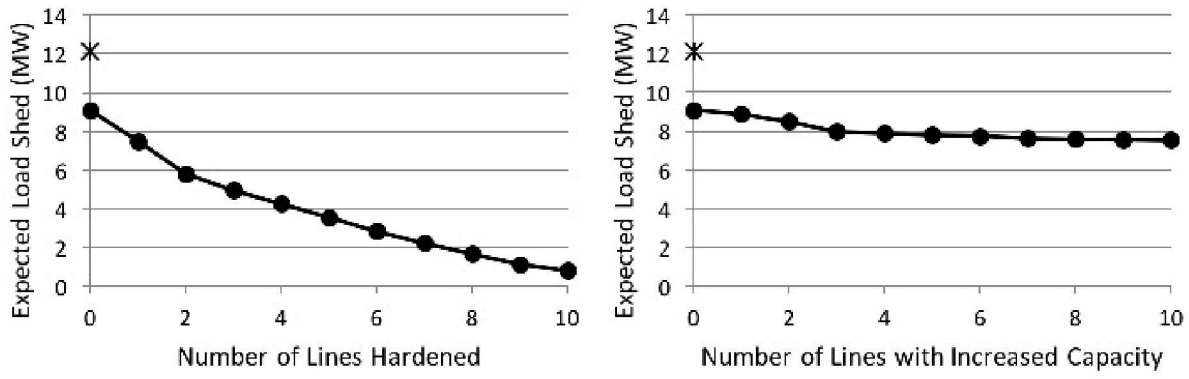

Fig. 2. The left and right panels illustrate results for THF and TCF, respectively, for case30. The y-axis indicates the expected load shed across all scenarios. The asterisk represents the *baseline*, which is the case where no preparation is done before the severe weather event. The points at zero hardened lines (or zero transmission lines with increased capacity) correspond to the RDF solution.

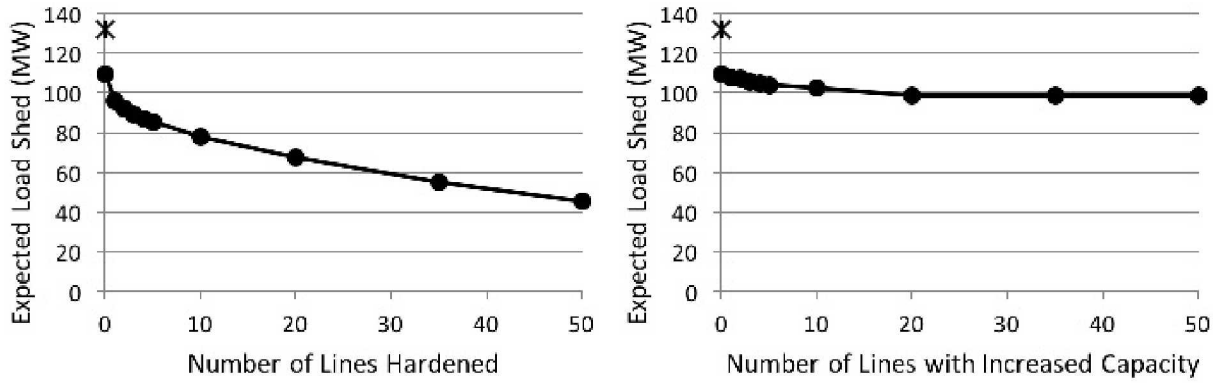

Fig. 3. The left and right panels illustrate results for THF and TCF, respectively, for case2383wp. The y-axis indicates the expected load shed across all scenarios. The asterisk represents the *baseline*, which is the case where no preparation is done before the severe weather event. The points at zero hardened lines (or zero transmission lines with increased capacity) correspond to the RDF solution.

therefore is immediately implementable by the system operator through operational adjustments.

The THF results indicate that line hardening can be very effective, with higher marginal gains from the initial investments. The left panels of Figures 4 and 5 show the incremental reduction in expected load shed decreasing with increasing number of lines hardened. For case30, the first two transmission lines hardened each reduce the expected load shed by over 13%. After the first two, there is a significant drop to about 7% followed by a continued gradual decline. Then for case2383wp, hardening just one transmission line reduces the expected load shed by 10%, followed by a significant decrease in which each transmission line hardened after the fifth decreases the expected load shed by less than 1.5%.

The TCF results indicate a slightly less effective strategy, as illustrated in the right panels of Figures 4 and 5. Our results for case30 indicate that doubling the transmission capacity of three transmission lines results in over 9% total reduction in expected load shed. For case2383wp, doubling the transmission capacity of five transmission lines results in approximately a 4.4% reduction in expected load shed. Increasing the capacity of transmission lines is clearly less effective than hardening per transmission line. Depending on

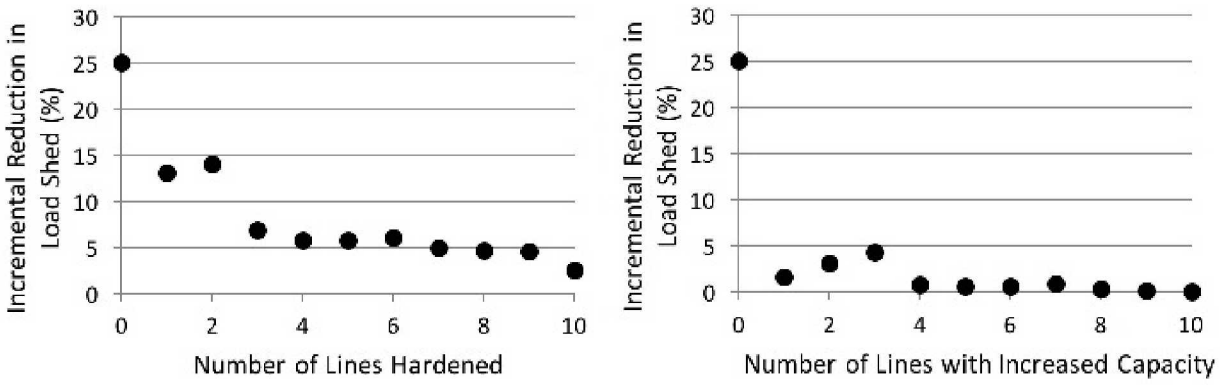

Fig. 4. Incremental reduction in expected load shed for each additional hardened line (left) and each additional line with increased capacity (right) for case30.

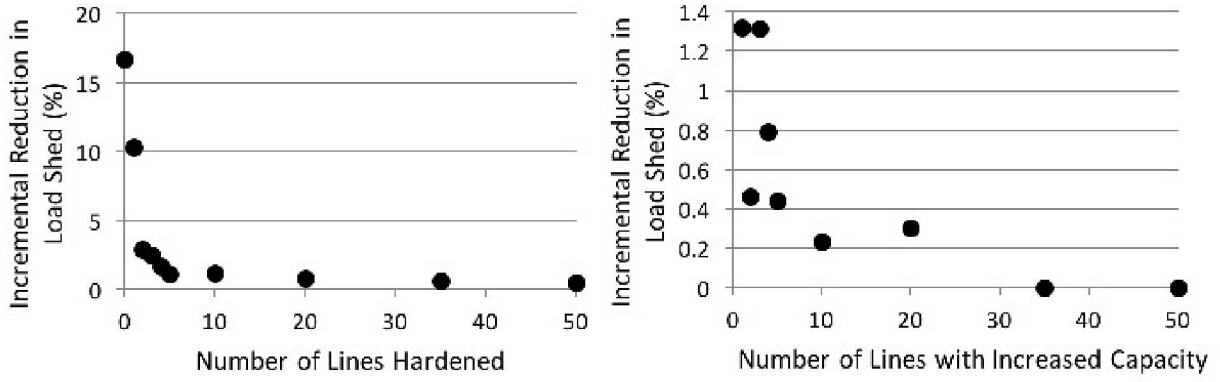

Fig. 5. Incremental reduction in expected load shed for each additional hardened line (left) and each additional line with increased capacity (right) for case2383wp.

the cost of increasing the transmission capacity of each of these lines, this could be combined with RDF and THF strategies for improved resilience.

4.1 Out-of-Sample Cross Validation

Even for a small test network such as case30, including all possible scenarios in the stochastic programming formulation is intractable. On average, the scenarios for case30 contained 7 transmission line outages. Over 22 million scenarios would be necessary to consider every combination of 7 outages. To demonstrate that only a small fraction of all possible scenarios is needed to obtain a high quality solution, a cross validation case study was performed with case30.

A set of 10 randomly sampled scenarios (different from the one hundred scenarios used above) was used to solve the RDF and THF problems. The solution was then used to evaluate the performance of the first stage solution on the original 100 scenarios used in Section 4. This process was then repeated with 30 and then 100 randomly sampled scenarios. The results are shown in Figure 6. Both the line labeled "True Scenarios" and the line in Figure 2 detail results when the stochastic programming problems are solved with the original 100 scenarios and the load shed in the second stage is evaluated on the same 100 scenarios. This

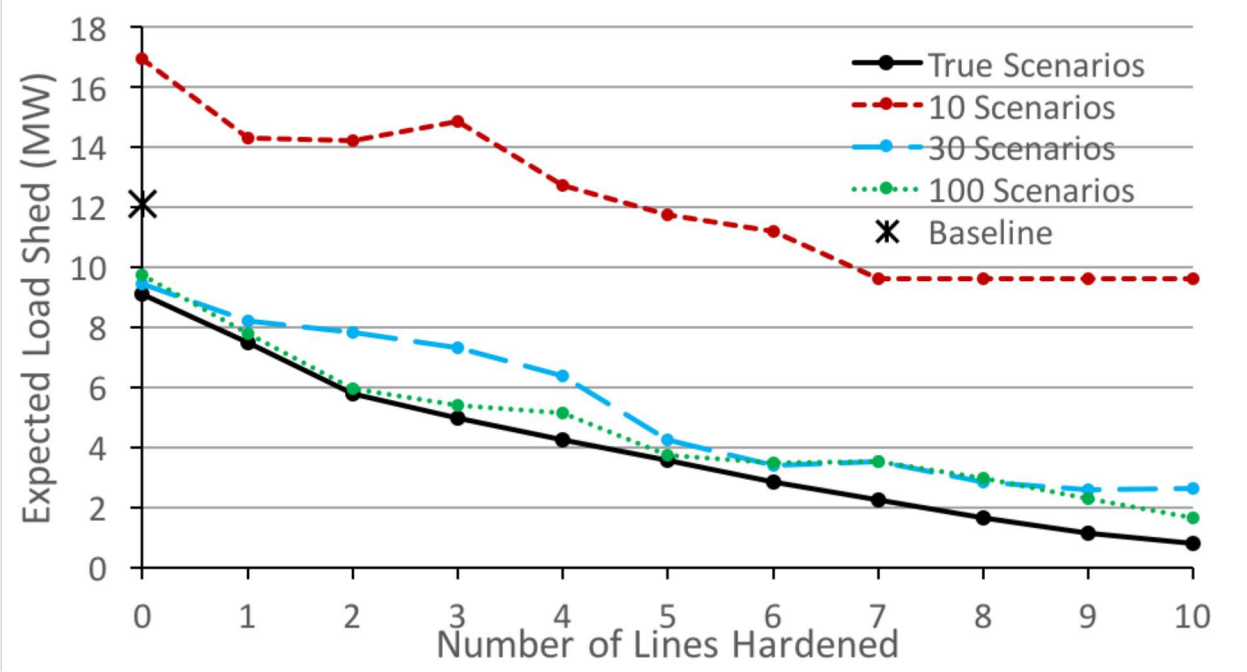

Fig. 6. Cross validation results for case30. The line labeled "True Scenarios" shows the expected load shed when the solution to the stochastic programming problem is evaluated on the same 100 scenarios used to solve the stochastic programming problem. The remaining lines show the expected load shed when the stochastic programming problem is solved with a different set of scenarios than those used to evaluate the expected load shed.

quantity represents the best possible performance.

Figure 6 shows that when only 10 scenarios are used to determine how to dispatch the generators in the first stage, the performance of the original 100 scenarios in the second stage is actually worse than the baseline. This is still true even after four transmission lines have been hardened, illustrating just how critical scenario selection is. The 30 scenario case performs significantly better, and the 100 scenario case performs almost as well as using the "True Scenarios." Thus, we obtained a high quality solution with less than 0.001% of all possible scenarios.

5 Conclusions and Future Work

Our proposed stochastic programming models for enhancing power systems resilience to extreme weather events shows promise, based on results obtained using synthetic and real world test systems. Specifically, relatively simple operational changes can significantly reduce the impact of extreme weather events, and hardening transmission can yield further reductions. Surprisingly, the non-capital approach (proactive re-dispatch) yields more significant reductions than the two capital approaches investigated.

Many modeling and algorithmic challenges remain. First of all, there are many resilience actions other than transmission line hardening and increasing transmission capacity that can be integrated with the proposed Resilient Dispatch Formulation (RDF). Such actions include transmission switching (i.e., network reconfiguration), investments in hardening current substations and generators, and development of new facilities including storage and microgrids. For example, recent studies have demonstrated that

microgrids can prevent cascading outages (Phase I) [7], mitigate performance degradation (Phase II) [15, 31], and improve restoration (Phase III) [5]. Moreover, these strategies can be considered in combination by considering, for example, information from the system operator or utility on budget availability, potential siting locations for hardening existing or installing new equipment, and possible operational actions.

Furthermore, the size of the stochastic programming problem increases with the product of the network size and the number of scenarios, making the solution of large scale systems computationally challenging. When the extensive form cannot be solved directly in the time allotted, stage-based or scenario-based decomposition methods such as progressive hedging [20] or Benders decomposition [4] can be applied.

6 Acknowledgements

Sandia National Laboratories is a multimission laboratory managed and operated by National Technology and Engineering Solutions of Sandia, LLC, a wholly owned subsidiary of Honeywell International, Inc., for the U.S. Department of Energy's National Nuclear Security Administration under contract DENA0003525. This work was funded by the U.S. Department of Energy's Office of Electricity, under the Advanced Grid Modeling (AGM) program, and by the U.S. Department of Homeland Security.

Disclaimer: This paper describes objective technical results and analysis. Any subjective views or opinions that might be expressed in the paper do not necessarily represent the views of the U.S. Department of Energy or the United States Government.

7 Notation

Sets

$\mathcal{A}$	Set of pairs (b, n) specifying adjacent buses;
$\mathcal{A}_s$	Set of pairs (b, n) specifying adjacent buses in scenario s, $\subseteq \mathcal{A}$;
$\mathcal{B}$	Set of all buses;
$\mathcal{G}$	Set of all generators;
$\mathcal{G}_b$	Set of generators at bus b, $\subseteq \mathcal{G}$;
$\mathcal{K}$	Set of all lines;
$\mathcal{K}_b$	Set of lines connected to bus $b \in \mathcal{B}$, $\subseteq \mathcal{K}$;
$\mathcal{K}_b^{\text{in}}$	Set of lines with bus $b \in \mathcal{B}$ as the "to" bus, $\mathcal{K}_b^{\text{in}} \subseteq \mathcal{K}$;
$\mathcal{K}_b^{\text{out}}$	Set of lines with bus $b \in \mathcal{B}$ as the "from" bus, $\mathcal{K}_b^{\text{out}}$;
$\mathcal{K}_s$	Set of lines out of service in scenario s, $\mathcal{K}_s \subseteq \mathcal{K}$;
$\mathcal{L}$	Set of 3-tuples denoting line k and interconnected buses b and n where $(b, n) \in \mathcal{A}$;
$\mathcal{L}_s$	Set of 3-tuples denoting lines out of service in scenario s, $\subseteq \mathcal{L}$; and
$\mathcal{S}$	Set of all scenarios.

Parameters

P_b^L	Real power load at bus b;
G_b^S	Shunt conductance at bus b;
$P_g^{G,\min}$	Minimum power output for generator g;
$P_g^{G,\max}$	Maximum power output for generator g;

$P_g^{G,R}$	Maximum power ramp rate for generator g;
$S_k^{\max}$	Maximum power flow on branch k;
T_k	Transformer tap ratio for branch k;
X_k	Reactance of branch k;
Ω_s	Probability of occurrence for scenario s;
Θ_k^{shift}	Transformer phase shift angle for branch k;
$\Theta_{(b,n)}^{\max}$	Maximum allowable voltage angle difference between buses b and n; and
M	"Big-M" parameter value.
Variables	
$p_b^{L,shed}$	Real power load shed at bus b;
p_g^G	Real power output at generator g;
$p_g^{G,cur}$	Real power curtailment at generator g;
p_k	Real power flow on line k;
δ_k	Binary indicator for whether line k is hardened;
γ_k	Binary indicator for whether the capacity of line k is increased; and
θ_b	Voltage angle at bus b.

References

[1] Adibi, M. and Fink, L. (1994). "Power system restoration planning." *IEEE Transactions on Power Systems*, 9(1), 22–28.

[2] Alguacil, N., Delgadillo, A., and Arroyo, J. M. (2014). "A trilevel programming approach for electric grid defense planning." *Computers & Operations Research*, 41, 282 – 290.

[3] Baldick, R., Chowdhury, B., Dobson, I., Dong, Z., Gou, B., Hawkins, D., Huang, H., Joung, M., Kirschen, D., Li, F., Li, J., Li, Z., Liu, C.-C., Mili, L., Miller, S., Podmore, R., Schneider, K., Sun, K., Wang, D., Wu, Z., Zhang, P., Zhang, W., and Zhang, X. (2008). "Initial review of methods for cascading failure analysis in electric power transmission systems ieee pes cams task force on understanding, prediction, mitigation and restoration of cascading failures." *2008 IEEE Power and Energy Society General Meeting - Conversion and Delivery of Electrical Energy in the 21st Century*, 1–8 (July).

[4] Benders, J. F. (1962). "Partitioning procedures for solving mixed-variables programming problems." *Numerische Mathematik*, 4(1), 238–252.

[5] Castillo, A. (2013). "Microgrid provision of blackstart in disaster recovery for power system restoration." *2013 IEEE International Conference on Smart Grid Communications (SmartGridComm)*, 534–539 (Oct).

[6] Chen, Q., Zhu, K., and McCalley, J. D. (2001). "Dynamic decision-event trees for rapid response to unfolding events in bulk transmission systems." *2001 IEEE Porto Power Tech Proceedings (Cat. No.01EX502)*, Vol. 2, 5 pp. vol.2–.

[7] Chen, X., Dinh, H., and Wang, B. (2010). "Cascading failures in smart grid - benefits of distributed generation." *2010 First IEEE International Conference on Smart Grid Communications*, 73–78 (Oct).

[8] Executive Office of the President (2013). "Economic benefits of increasing electric grid resilience to weather outages." *Report no.*, Technical report.

[9] Fan, N., Izraelevitz, D., Pan, F., Pardalos, P. M., and Wang, J. (2012). "A mixed integer programming approach for optimal power grid intentional islanding." *Energy Systems*, 3(1), 77–93.

[10] Guikema, S. D., Quiring, S. M., and Han, S.-R. (2010). "Prestorm estimation of hurricane damage to electric power distribution systems." *Risk analysis*, 30(12), 1744–1752.

[11] Gurobi Optimization, L. (2018). "Gurobi optimizer reference manual, <http://www.gurobi.com>.

[12] Hart, W. E., Laird, C. D., Watson, J.-P., Woodruff, D. L., Hackebeil, G. A., Nicholson, B. L., and Siirola, J. D. (2017). *Pyomo - optimization modeling in python*, Vol. 67. Springer.

[13] House, T. W. (2013). "Presidential policy directive – critical infrastructure security and resilience (February). Accessed: 2016-09-19.

[14] ILOG, I. (2009). *IBM ILOG CPLEX V12.1: User's manual for CPLEX* (01).

[15] Liu, X., Shahidehpour, M., Li, Z., Liu, X., Cao, Y., and Bie, Z. (2017). "Microgrids for enhancing the power grid resilience in extreme conditions." *IEEE Transactions on Smart Grid*, 8(2), 589–597.

[16] Ouyang, M. and Duenas-Osorio, L. (2014). "Multi-dimensional hurricane resilience assessment of electric power systems." *Structural Safety*, 48, 15–24.

[17] Panteli, M. and Mancarella, P. (2015). "Influence of extreme weather and climate change on the resilience of power systems: Impacts and possible mitigation strategies." *Electric Power Systems Research*, 127, 259–270.

[18] Panteli, M., Pickering, C., Wilkinson, S., Dawson, R., and Mancarella, P. (2017a). "Power system resilience to extreme weather: Fragility modeling, probabilistic impact assessment, and adaptation measures." *IEEE Transactions on Power Systems*, 32(5), 3747–3757.

[19] Panteli, M., Trakas, D. N., Mancarella, P., and Hatziargyriou, N. D. (2017b). "Power systems resilience assessment: hardening and smart operational enhancement strategies." *Proceedings of the IEEE*, 105(7), 1202–1213.

[20] Rockafellar, R. T. and Wets, R. J.-B. (1991). "Scenarios and policy aggregation in optimization under uncertainty." *Mathematics of Operations Research*, 16(1), 119–147.

[21] Salmeron, J., Wood, K., and Baldick, R. (2004). "Analysis of electric grid security under terrorist threat." *IEEE Transactions on Power Systems*, 19(2), 905–912.

[22] Shao, C., Shahidehpour, M., Wang, X., Wang, X., and Wang, B. (2017). "Integrated planning of electricity and natural gas transportation systems for enhancing the power grid resilience." *IEEE Transactions on Power Systems*, 32(6), 4418–4429.

[23] Song, H. and Kezunovic, M. (2007). "A new analysis method for early detection and prevention of cascading events." *Electric Power Systems Research*, 77(8), 1132 – 1142.

[24] Sun, W., Liu, C.-C., and Zhang, L. (2011). "Optimal generator start-up strategy for bulk power system restoration." *IEEE Transactions on Power Systems*, 26(3), 1357–1366.

[25] Tan, J. C., Crossley, P. A., McLaren, P. G., Gale, P. F., Hall, I., and Farrell, J. (2002). "Application of a wide area backup protection expert system to prevent cascading outages." *IEEE Transactions on Power Delivery*, 17(2), 375–380.

[26] Vaiman, M., Hines, P., Jiang, J., Norris, S., Papic, M., Pitto, A., Wang, Y., and Zweigle, G. (2013). "Mitigation and prevention of cascading outages: Methodologies and practical applications." *Power and Energy Society General Meeting (PES), 2013 IEEE*, IEEE, 1–5.

[27] Wang, Q., Watson, J. P., and Guan, Y. (2013). "Two-stage robust optimization for n-k contingency-constrained unit commitment." *IEEE Transactions on Power Systems*, 28(3), 2366–2375.

[28] Wang, X. and Vittal, V. (2004). "System islanding using minimal cutsets with minimum net flow." *IEEE PES Power Systems Conference and Exposition, 2004.*, 379–384 vol.1 (Oct).

[29] Wang, Y., Chen, C., Wang, J., and Baldick, R. (2016). "Research on resilience of power systems under natural disasters?a review." *IEEE Transactions on Power Systems*, 31(2), 1604–1613.

[30] Wang, Y., Shahidehpour, M., Lai, L. L., Huang, L., Yuan, H., and Xu, F. Y. (2018). "Resilience-constrained hourly unit commitment in electricity grids." *IEEE Transactions on Power Systems*.

[31] Wang, Z. and Wang, J. (2015). "Self-healing resilient distribution systems based on sectionalization into microgrids." *IEEE Transactions on Power Systems*, 30(6), 3139–3149.

[32] Watson, J.-P., Guttromson, R., Silva-Monroy, C., Jeffers, R., Jones, K., Ellison, J., Rath, C., Gearhart, J., Jones, D., Corbet, T., et al. (2014). "Conceptual framework for developing resilience metrics for the electricity, oil, and gas sectors in the united states." *Sandia National Laboratories, Albuquerque, NM (United States), Tech. Rep*.

[33] Wu, X. and Conejo, A. J. (2017). "An efficient tri-level optimization model for electric grid defense planning." *IEEE Transactions on Power Systems*, 32(4), 2984–2994.

[34] Zare, M., Abbaspour, A., Fotuhi-Firuzabad, M., and Moeini-Aghtaie, M. (2017). "Increasing the resilience of distribution systems against hurricane by optimal switch placement." *Electrical Power Distribution Networks Conference (EPDC), 2017 Conference on*, IEEE, 7–11.

[35] Zima, M. and Andersson, G. (2004). "Wide area monitoring and control as a tool for mitigation of cascading failures." *2004 International Conference on Probabilistic Methods Applied to Power Systems*, 663–669 (Sept).

[36] Zimmerman, R. D. and Murillo-Sanchez, C. E. (2015). "Matpower 5.1-user's manual." *Power Systems Engineering Research Center (PSERC)*.